

Self-Assembling Peptide Nanofibers Coupled with Neuropeptide Substance P for Bone Tissue Engineering

Su Hee Kim, MS,^{1,2,*} Woojune Hur, MS,^{3,4,*} Ji Eun Kim, MS,^{1,2} Hye Jeong Min, MS,^{3,4} Sukwha Kim, MD, PhD,³ Hye Sook Min, MD, PhD,⁵ Byeung Kyu Kim, PhD,^{3,4} Soo Hyun Kim, PhD,^{1,2} Tae Hyun Choi, MD, PhD,^{3,4} and Youngmee Jung, PhD^{1,6}

The number of patients requiring flat bone transplantation continues to increase worldwide. Cell transplantation has been successfully applied clinically; however, it causes another defect site and the time requirements to harvest cells and expand them are considerable. In this study, KLD12/KLD12-SP (KLD12+KLD12-substance P [SP]) was designed to mimic endogenous tissue-healing processes. The structures of KLD12, KLD12-SP, and KLD12/KLD12-SP were observed by transmission electron microscopy and circular dichroism spectra. KLD12/KLD12-SP nanofibers (5–10 nm) were created under physiological conditions by formation of a β -sheet structure. The ability of mesenchymal stem cells (MSCs) to recruit KLD12/KLD12-SP was observed by using an *in vivo* fluorescence imaging system. Labeled human bone marrow stromal cells supplied via an intravenous injection were recruited to the scaffold containing KLD12/KLD12-SP. Polylactic acid/beta-tricalcium phosphate (PLA/ β -TCP) scaffolds filled with KLD12/KLD12-SP were applied to repair calvarial defects. The composite constructs (groups: defect, PLA/ β -TCP, PLA/ β -TCP/KLD12, and PLA/ β -TCP/KLD12/KLD12-SP) were implanted into rat defect sites. Bone tissue regeneration was evaluated by observing gross morphology by hematoxylin and eosin and Masson's trichrome staining at 12 and 24 weeks after surgery. Gross morphology showed that the defect site was filled with new tissue that was integrated with host tissue in the KLD12/KLD12-SP group. In addition, from the staining data, cells were recruited to the defect site and lacunae structures formed in the KLD12/KLD12-SP group. From these results, the PLA/ β -TCP+KLD12/KLD12-SP composite construct was considered for enhancement of bone tissue regeneration without cell transplantation.

Introduction

PATIENTS REQUIRING FLAT bone transplantation continue to increase worldwide. Repair of cranio-maxillofacial deformation or calvarial bone defects caused by hereditary diseases, severe trauma, resection, or tumors still has limitations.¹ Numerous studies on various biomaterials and cell-based therapies have sought to regenerate bone tissue. Many types of bioceramics and growth factors have been used with biodegradable polymer scaffolds for osteogenesis of mesenchymal stem cells (MSCs) or preosteoblasts.^{1,2} Coating or mixing of hydroxyapatite or β -TCP with bone substitutes enhances bone regeneration due to their osteoconductivity

and osteoinductivity.³ It has also been reported that MSCs derived from bone marrow or adipose tissue can improve regeneration efficiency. These MSCs contribute to tissue regeneration while forming new tissues by differentiation and secretion of various cytokines.^{4,5}

Stem cell-based therapy has been used to treat bone injury and may be one of the best approaches for bone regeneration. However, although cell transplantation results provide good prognosis, there are some obstacles such as cell source limitations, invasiveness, time requirements and the cost of expansion.⁶ To overcome these limitations, many studies have tried to mimic endogenous wound-healing processes instead of using stem cell transplantation. When tissue is

¹Center for Biomaterials, Biomedical Research Institute, Korea Institute of Science and Technology, Seoul, Korea.

²NBIT, KU-KIST Graduate School of Converging Science and Technology, Korea University, Seoul, Korea.

³Department of Plastic and Reconstructive Surgery, Institute of Human-Environment Interface Biology, Institute of Dermatologic Science, College of Medicine, Seoul National University, Seoul, Korea.

⁴Biomedical Research Institute, Seoul National University Hospital, Seoul, Korea.

⁵Department of Preventive Medicine, Graduate School of Public Health, Seoul National University, Seoul, Korea.

⁶Department of Biomedical Engineering, University of Science and Technology (UST), Seoul, Korea.

*These two authors contributed equally to this work.

damaged, various signaling factors are secreted to initiate the stem cell mobilization process. Signaling molecules such as IL-3, IL-7, IL-8, IL-12, and SDF-1 as well as VEGF and IGF can induce stem cell mobilization through chemotherapeutic agents. Cell homing is a very important mechanism for survival, proliferation, and differentiation of tissue-specific progenitor cells in bone marrow. Some studies have shown that SDF-1 α can be used as a therapeutic stem cell homing factor in myocardial infarction. These studies confirmed that cardiac function is improved by increasing stem cell homing, angiogenesis, and anti-fibrosis.⁷⁻¹¹ Recently, the effects of substance P (SP) on wound-healing processes have been reported in several articles. SP is an 11-amino-acid neuropeptide secreted from the peripheral terminals of sensory nerve fibers. It is an injury-inducible factor that acts to induce mobilization of CD29⁺ stromal-like cells in wound-healing processes. It was reported that SP accelerates wound healing in an alkali burn corneal injury model by its systemic action.^{12,13} It was also confirmed that controlled release of SP induces recruitment of circulating cells with angiogenic activities from the blood to the injury site, resulting in enhanced angiogenesis.^{14,15} Furthermore, SP has been used for treatment of cardiovascular disease and limb ischemia.^{16,17} To improve the effect of SP over a long period of time, studies regarding controlled release systems have been performed.¹⁴

In our previous work, self-assembling peptide (SAP) with a sequence of Ac-KLDLKLKLDL-NH₂ (KLD12) was demonstrated to be a good delivery system for MSCs in a rat osteoarthritis model.^{18,19} Under physiological conditions, SAP forms a network of stable β -sheet-rich nanofibers with a diameter between 5 and 10 nm.²⁰⁻²² This structure resembles *in vivo* 3D nanostructured environments such as collagen hierarchical structures that promote adhesion, proliferation, and differentiation of cells in their surrounding environment.^{23,24}

In this study, KLD12/KLD12-SP was designed by coupling KLD12 to SP. We presupposed that KLD12/KLD-SP increases the number of circulating MSCs in the body, and immobilizes and recruits them to the injured site. It also improves tissue regeneration by enhancing cell attachment, proliferation, and differentiation. As we confirmed the effects of polylactic acid/beta-tricalcium phosphate (PLA/ β -TCP) scaffold in our previous work,²⁵ we expected that the composite scaffold enhances osteogenic differentiation of recruited MSCs by increasing alkaline phosphatase (ALP) activity during tissue regeneration in the present system. This modified KLD12 peptide was evaluated for its ability to recruit MSCs and promote bone regeneration. In addition, the structural characteristics of KLD12/KLD12-SP were also investigated. KLD12/KLD12-SP was combined with a PLA/ β -TCP porous scaffold and applied in a rat calvarial defect model. We hypothesized that this KLD12/KLD12-SP+PLA/ β -TCP construct would have the ability to recruit MSCs and, consequently, promote bone regeneration.

Materials and Methods

Peptide synthesis and preparation

The peptides with a sequence of Ac-KLDLKLKLDL-NH₂ (KLD12) and Ac-KLDLKLKLDLGRPKPQQFF GLM-NH₂ (KLD12-SP) were synthesized (Pepton) and

dissolved in 295 mM sucrose solution to produce 1% (wt/vol) peptide gel. The solution was then mixed with phosphate-buffered saline (PBS) and sonicated for 30 min to prepare 0.5% KLD12 and KLD12-SP. For KLD12/KLD12-SP, KLD12 and KLD12-SP were mixed (70:1, vol/vol). The KLD12/KLD12-SP contained 5 μ g of SP in a sample.

Structural characterization

The structure of the SAP gel was examined by transmission electron microscopy (TEM). The samples were diluted in distilled water to a working concentration of 0.01% and stained with 2% uranyl acetate. To identify the structure of the peptide gel, circular dichroism (CD) spectra of SAP were obtained using a spectro-polarimeter (JASCO, Inc.). KLD12, KLD12-SP, and KLD12/KLD12-SP were prepared by diluting peptide solutions in distilled water to working concentrations of 0.02% (wt/vol), and then incubated at room temperature overnight. For CD spectra measurements, samples were added to a quartz cuvette with a 1-mm path length (Hellam Standard Cuvet 110QS (Quartz Suprasil); Hellma Analytics).⁶

Preparation of the PLA/ β -TCP scaffold

The PLA/ β -TCP composites (diameter=9 mm/thickness=2 mm) were prepared by the sintering method as described in our previous work.³

Before performing the surgery, the PLA/ β -TCP scaffold was prewetted in culture medium for 4 h. Next, peptide gels (70 μ L) were injected into each scaffold. The total amount of SP was 5 μ g in the KLD12/KLD12-SP group.

In vitro CD29⁺ cell migration assay

Cell migration assays were performed using a trans-well system (8- μ m pores, cell culture insert; SPL) to examine the ability of SP to mobilize MSCs. Rat bone marrow stromal cells (BMSCs) (1×10^4 cells) were seeded on the upper chambers. The cells were grown and maintained in serum-free medium for 48 h to allow synchronization. The lower chamber was then filled with 400 μ L of 1% fetal bovine serum Dulbecco modified Eagle medium/F12 media containing sucrose (1%; Sigma), KLD12 (200 μ L, 5 mg/mL), KLD12/KLD12-SP (KLD12:KLD-SP=200 μ L:1 μ L), or soluble SP (5 μ g). After 48 h, the membranes were washed with PBS, fixed with 4% paraformaldehyde solution for 20 min, permeabilized with cold methanol for 15 min, and then stained with crystal violet solution (Sigma). The cell culture inserts were removed from each well, and the upper parts of the membranes were wiped with a cotton-tipped swab to remove nonmigrated cells. Migrated cells were observed with a microscope after staining.²⁶

In vivo real-time human BMSCs recruiting assay

All animals (balb/c, 7 week-old, male, 20–30 g; Nara Biotech) were cared for according to methods approved by the Institutional Animal Care and Use Committee (IACUC, 2009-01-5254-002) at Korea Institute of Science and Technology. For subcutaneous implantation, temporary anesthesia was performed by an intramuscular (IM) injection with a cocktail of zolazepam and tiletamine (0.3 mL/kg; Zoletil[®]; Virbac) and xylazine (0.1 mL/kg, Rompun[®]; Bayer).

Human BMSCs (hBMSCs) were supplied from Yonsei University Hospital after approval by the institutional review board. hBMSCs were labeled with near-infrared nanoparticles (NEO-LIVE Magnoxide 675, ex/em=675/700) according to the manufacturer's instructions.

PLA scaffolds prepared by the sintering method (porosity = 90%, pore size = 300–500 μm , diameter = 5 mm, thickness = 3 mm, disk type) containing KLD12/KLD12-SP, KLD12 or PBS were implanted subcutaneously into nude mice ($n=3$), and then hBMSCs (1×10^6 cells/200 μL of PBS) were injected into the tail vein of the mice. After surgery, the movement of injected cells was tracked at every 2–3 days for 6 weeks by using an *in vivo* fluorescence imaging system (I-VIS spectrum; Caliper Life Sciences). Acquired images were processed with an image analysis program (Image J; NIH) for calculating the optical density and stained area. Nuclei were counterstained with 4',6-diamidino-2-phenylindole (DAPI Molecular Probes). To confirm that MSCs were recruited *in situ* 2 weeks after surgery, the explanted samples were stained with CD29 and CD90 antibodies (1:1000 and 1:500; Abcam) that served as MSC markers.

Surgery of calvarial defect model

All animals (SD-RAT, male, 7 weeks, 200–300 g; Koatech) were cared for according to methods approved by the Institutional Animal Care and Use Committee (IACUC No. 11-0301) at Seoul National University Hospital. For calvarial defect, temporary anesthesia was performed by IM injection with a cocktail of zolazepam and tiletamine (0.3 mL/kg, Zoletil; Virbac) and xylazine (0.1 mL/kg, Rom-

pun; Bayer). The calvarial bone was exposed through a skin incision (~ 4 cm in length) and defected to a diameter of 8 mm using a trephine bur (TPHB-B8; OSUNG). The bone was removed, and the prepared samples were implanted to investigate bone regeneration. Each implant was observed after 12 and 24 weeks by histological staining analysis. For calvarial defect surgery, the rats were randomly allocated into four groups ($n=2$) as follows: Group 1 = scaffold only; Group 2 = scaffold + KLD12; Group 3 = scaffold + KLD12/KLD12-SP; and Group 4 = control (received nothing).⁴

Histological analysis and immunofluorescence staining

At 12 and 24 weeks, the implanted animals were sacrificed and defected bone was sampled. The sampled tissues were sectioned at 6–7 μm thickness and then stained with hematoxylin and eosin (H&E) or Masson's trichrome (MT) stains. To investigate MSC homing to the injury site during bone regeneration, samples were stained with the MSC markers CD29 and CD90. In addition, the samples were stained with type 1 collagen (1:500; Abcam) and osteocalcin (1:500; Abcam) antibodies to evaluate the differentiation of cells recruited to the defect site during bone tissue regeneration.

Statistical analysis

All the samples were assayed in triplicate, and the results obtained were expressed in standard deviation (SD) above and below the mean \pm SD. All statistical analyses were carried out using the *t*-test. A result was considered statistically significant when the *p*-value was less than 0.05.

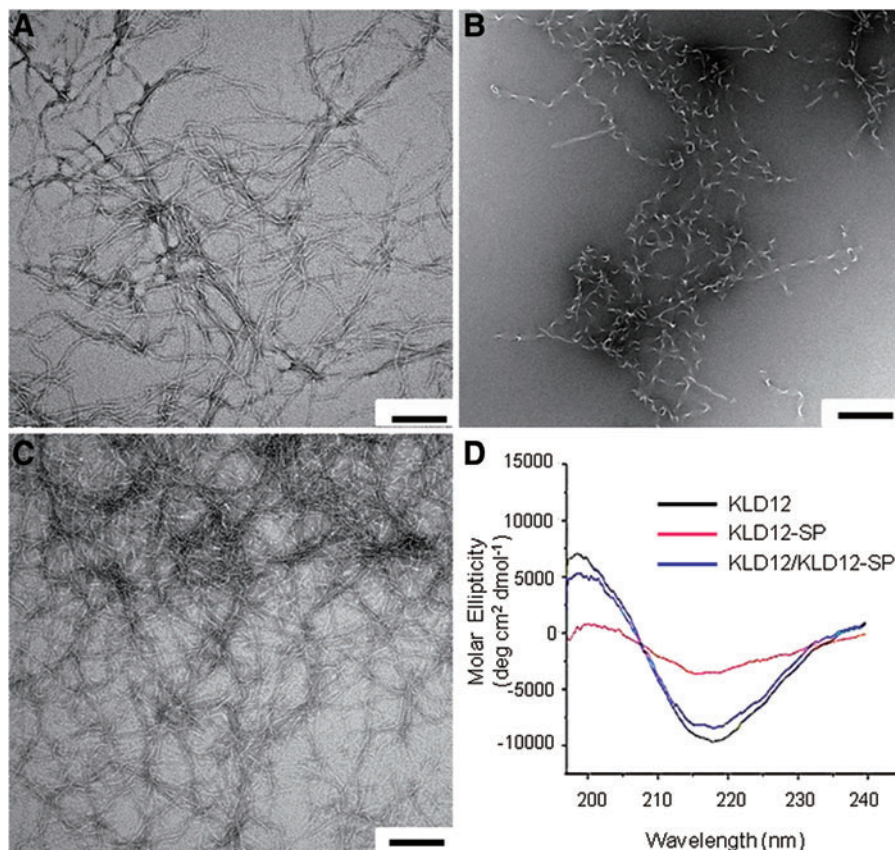


FIG. 1. Structural analysis. Transmission electron microscopy image of (A) KLD12, (B) KLD12-SP, and (C) bioactive KLD12. (D) Circular dichroism spectra of various peptides. Scale bar: 100 nm. SP, substance P. Color images available online at www.liebertpub.com/tea

Results and Discussion

Structural analysis

The nanostructures of the SAP hydrogels were observed by TEM. From the results, we confirmed that KLD12 was composed of ~5–10 nm nanofibers, but KLD12-SP formed more of a random structure and did not form nanofibers (Fig. 1A, B). Figure 1C shows that the image of KLD12/KLD12-SP is broadly similar to the image of KLD12. To identify the secondary structure of the peptide hydrogels, CD spectra of KLD12, KLD12-SP, and KLD12/KLD12-SP were analyzed. The results revealed that the molecular ellipticity ($\text{deg}\cdot\text{cm}^2/\text{dmol}$) of KLD12 was a network of β -sheet structures in a region of 195–216 nm (Fig. 1D). KLD12 peptide with a sequence of Ac-KLDLKLKLDL-NH₂ consists of alternating hydrophilic residues (Lysine and Aspartic acid) and hydrophobic residues (Leucine). This oligopeptide can form stable β -sheets in the presence of salt ions. Since this peptide is short and simple, it can be self-assembled through weak interactions such as hydrogen bonds, ionic bonds, hydrophobic interactions, and van der Waals interactions. Through such structural changes, KLD12 peptides become nanofibers.^{22,23} For KLD12/KLD12-SP, the CD spectrum showed results similar to the TEM images of KLD12. However, KLD12-SP had a random structure that was widely different from that of the spectrum for KLD12 and KLD12/KLD12-SP. KLD12-SP consists of 24 amino acids. Since the part consisting of SP is not an alternating sequence and relatively long, it may interfere with intermolecular interactions. This leads to a random structure of the peptide. KLD12/KLD12-SP is a mixture of KLD12 and KLD12-SP, with KLD12-SP representing 0.5 vol%. Therefore, the effect of KLD12-SP on formation of the nanofibers is infinitesimal. Thus, the CD spectra data indicated that KLD12 and KLD12/KLD12-SP form very stable β -sheet structures.

In vitro MSC migration assay

In this study, we tried to mimic this endogenous recruiting system for bone regeneration. Trans-well assays were performed for the *in vitro* migration assay to compare the chemotactic ability of KLD12/KLD12-SP with that of soluble SP. The results confirmed that many cells migrated through the 8- μm membrane pores by the action of KLD12/KLD12-SP or soluble SP compared with the negative control (sucrose solution). As shown in Figure 2A, cells seldom migrated in the control group. In contrast, cells migrated to the lower surface of the membrane in the other groups. According to these results, the soluble SP group had the greatest number of migrating cells. The burst effect of soluble SP may cause initial cell migration. However, although the average number of migrated cells in the soluble SP group was more than that of the KLD12/KLD12-SP group, there was no significant difference between the groups. From this study, we confirmed that KLD12/KLD12-SP appeared to have the same ability to recruit MSCs as soluble SP.

In vivo MSC recruitment and real-time MSC tracking assay

One of the many roles of SP is to participate in wound-healing processes by recruiting MSCs. To investigate the

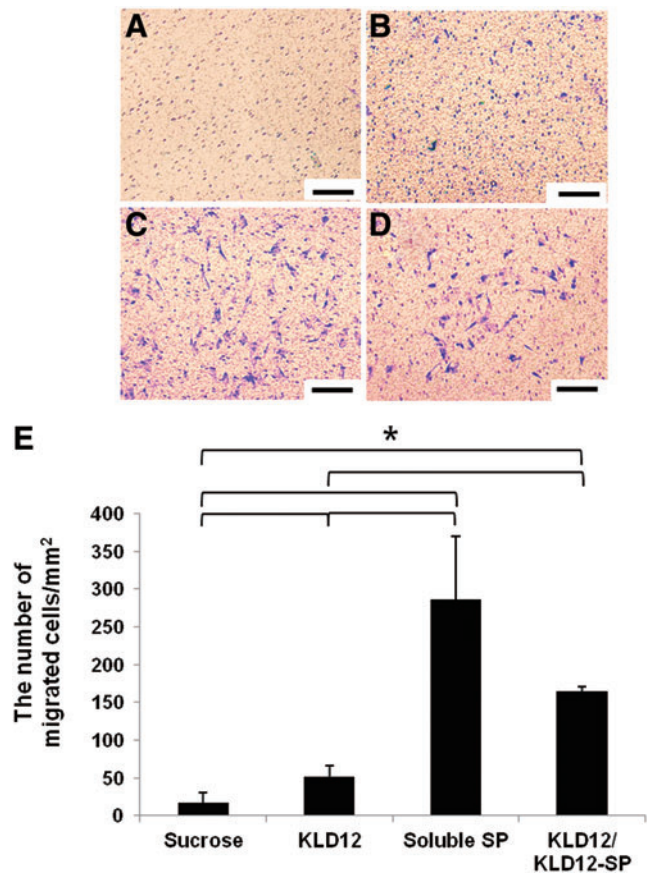


FIG. 2. *In vitro* MSC migration assay. (A) Sucrose (negative control). (B) KLD12. (C) Soluble SP. (D) Bioactive KLD12. (E) Quantitative analysis (* $p < 0.05$). Scale bar: 100 μm . MSCs, mesenchymal stem cells. Color images available online at www.liebertpub.com/tea

mechanism underlying the effect of SP *in vivo*, MSCs were tracked in real time. At the beginning of cell tracking, MSCs were detected in the lung and liver until 2 weeks after surgery. However, circulating cells started gathering on the implanted scaffold after 3 weeks. Figure 3A shows that MSCs were continuously recruited for 6 weeks. As shown in Figure 3A, the KLD12/KLD12-SP group showed the best recruiting ability. According to quantitative analysis, the optical intensity of the KLD12/KLD12-SP group was 6.42 times higher than that of the PBS group and 2.02 times higher than that of the KLD12 group. Although the KLD12 group did not contain the MSC recruiting factor, peptide hydrogels provided a good microenvironment for cell attachment and proliferation. Therefore, partially migrated cells may be maintained in this material. After 6 weeks, the implanted scaffolds were harvested and observed by confocal microscopy. Figure 3E shows that a large number of labeled MSCs were recruited to the scaffold containing KLD12/KLD12-SP.

For successful wound healing, initial events such as MSC recruitment, cytokine secretion, and angiogenesis are very important. However, we could not observe recruitment of MSCs in the early stage of implantation by *in vivo* tracking in real time. Thus, to confirm that MSCs were recruited within 2 weeks after implantation without skin interference,

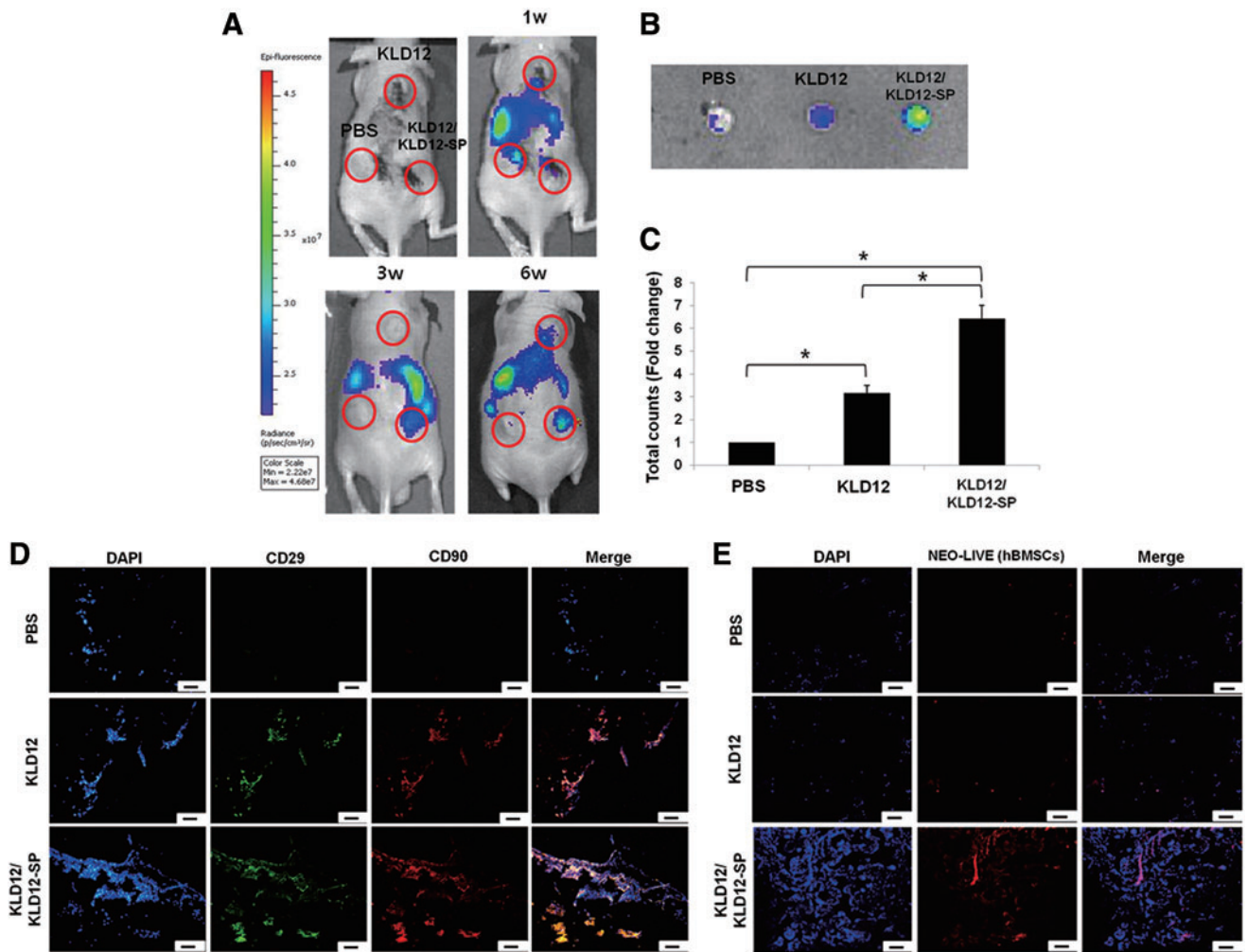


FIG. 3. (A) *In vivo* real-time hBMSC recruiting assay. Movement of labeled hBMSCs to the scaffolds containing bioactive KLD12, KLD12, or PBS at 6 weeks. (B) Optical images of the scaffolds explanted after 6 weeks. (C) Quantitative analysis of optical intensity ($*p < 0.05$). (D) MSC recruitment of bioactive KLD12-SP peptides. Representative images of the scaffolds containing bioactive KLD12, KLD12, or PBS after 2 weeks (nonlabeled hBMSCs were used). (E) Neo-live labeled hBMSCs at 6 weeks after subcutaneous implantation of the scaffolds. Scale bar: 100 μ m. hBMSCs, human bone marrow stromal cells; PBS, phosphate-buffered saline. Color images available online at www.liebertpub.com/tea

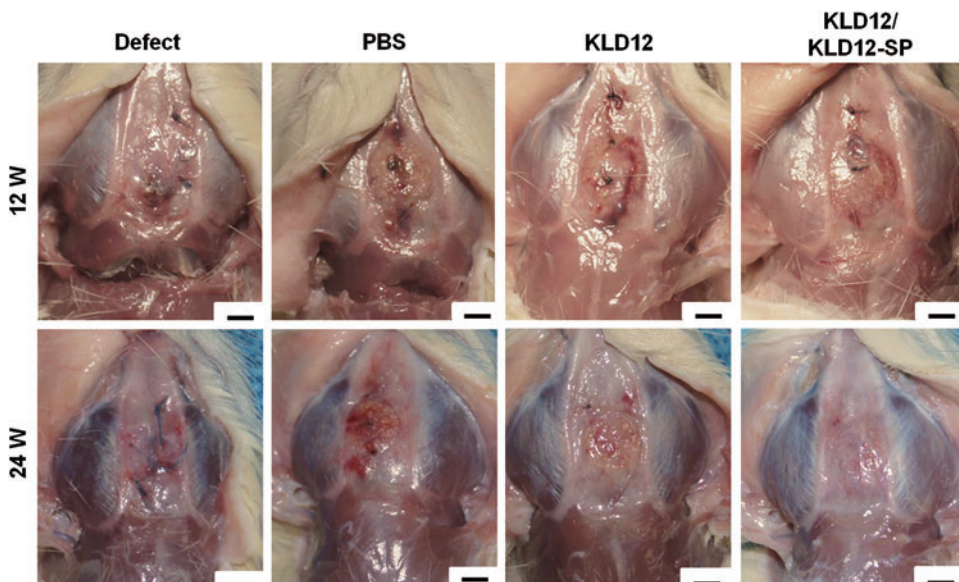
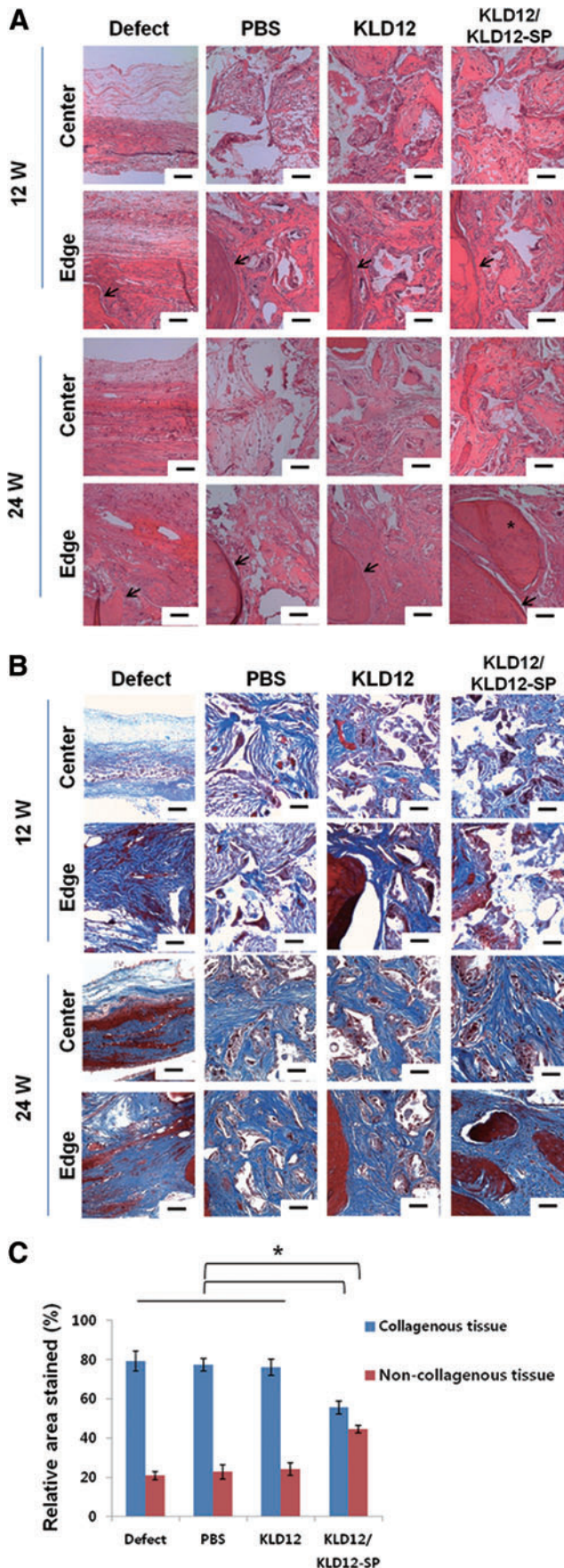


FIG. 4. Bone reconstruction of each group in the calvarial model at 12 and 24 weeks. Scale bar: 3 mm. Color images available online at www.liebertpub.com/tea



the scaffolds containing KLD12/KLD12-SP, KLD12, or PBS were explanted at 2 weeks after implantation and then examined. Many cells expressing CD29 and CD90 were observed within the scaffolds containing KLD12/KLD12-SP (Fig. 3D). From these results, we confirmed the recruiting and homing effects of KLD12/KLD12-SP on MSCs.

Bone regeneration in a rat calvarial defect model

In our previous work, we confirmed that PLA/ β -TCP scaffolds enhance bone regeneration in a rabbit ulna bone defect model.^{3,25,27-30} In this study, we combined PLA/ β -TCP scaffolds to KLD12/KLD12-SP, KLD12 or PBS for mechanical strength and osteoinductivity. For successful tissue regeneration, matching of scaffold degradation rate with tissue regeneration rate is important. However, since a PLA/ β -TCP scaffold has a low degradation rate, when only the scaffold was implanted (PBS group), bone formation and integration quality were not as high as the defect group. Numerous research studies have reported that peptide gel improves cell migration, attachment, and differentiation in the 3D environment such as collagen fibers. The KLD12 group showed higher cell migration to the injured site than the PBS group; however, it was not enough to recover the tissue. From the gross morphology at 12 weeks, the defects implanted with the scaffold containing KLD12/KLD12-SP were filled with newly formed bone tissues, which integrated well with host bone tissue (Fig. 4). This may have resulted from the migration of MSCs to the defect site by the action of SP. However, degradation of the scaffold was too slow; therefore, the PLA/ β -TCP scaffold disturbed bone growth at the beginning of tissue regeneration.

From the gross morphology at 24 weeks, the defect site in the PBS group was not filled and/or fully recovered. However, for the KLD12 group, newly formed bone tissues covered the defect and the interface between the defect and host tissues was well integrated at 24 weeks compared with 12 weeks. The KLD12/KLD12-SP group showed full recovery at the defect site as evident by the formation of new bone tissue that was well integrated with host tissue.

Histological analysis of in vivo samples

H&E staining at 12 weeks after implantation showed that the defect group had the smallest number of cells recruited to the injury site (Fig. 5A). In addition, a similar amount of cells were observed on the edge of the scaffolds in all groups except the defect group. However, a relatively large number of cells were recruited to the center of the scaffolds in the

FIG. 5. (A) Hematoxylin and eosin staining for each group (defect, PBS, KLD12, and bioactive KLD12) of the calvarial model at 12 and 24 weeks. The images of all groups were taken on the edge and center (*arrow*: interface between host tissue and new tissue, *asterisk*: new bone tissue [lacunae structure]). (B) Masson's trichrome staining for each group (defect, PBS, KLD12, and bioactive KLD12) of the calvarial model at 12 and 24 weeks. Photographs of the edge and center were taken for all groups. (C) Quantitative analysis of the stained area (collagenous and noncollagenous tissue) ($*p < 0.05$). Scale bar: 50 μ m. Color images available online at www.liebertpub.com/tea

KLD12 and KLD12/KLD12-SP groups compared with the defect and PBS groups.

The images of samples stained with H&E at 24 weeks showed that the number of cells and area of newly formed tissues increased compared with those at 12 weeks. However, since the number of recruited cells was not sufficient, the defects were not fully covered with new tissue in the defect and PBS groups. In contrast, for the KLD12 and KLD12/KLD12-SP groups, the defect site was mostly filled with newly formed tissue and bone tissue formation was evident in the edge of the scaffold where a lacuna structure was observed. Furthermore, an increase in calcified tissues and mature bone tissue within lacunae were observed on the edge of the scaffold containing KLD12/KLD12-SP compared with the KLD12 group. Subsequently, the levels of collagen deposited in the tissue were examined by measuring the integrated optical density of trichrome-stained images. Mature bone tissue has non-collagenous regions containing a lacuna structure that is

surrounded with osteoid. Therefore, we evaluated mature bone tissue formation by measuring the area of non-collagenous tissue. A graph quantifying these results is shown in Figure 5C. The blue bar represents the area of the collagenous regions, and the red bar represents the area of osteogenic cells and bone matrix regions. The bony area in the KLD12/KLD12-SP group was much higher than that of the other groups.

Immunofluorescence staining of *in vivo* samples

To investigate MSCs homing to the injury site and bone tissue regeneration during bone regeneration, MSC markers and osteogenic markers were observed by immunofluorescence staining. Figure 6 shows that a few MSCs were observed at 12 and 24 weeks, and the amount of stained MSCs was similar among all groups. However, there was more type 1 collagen and osteocalcin in the KLD12/KLD12-SP group compared with that of the other groups (Fig. 7). On

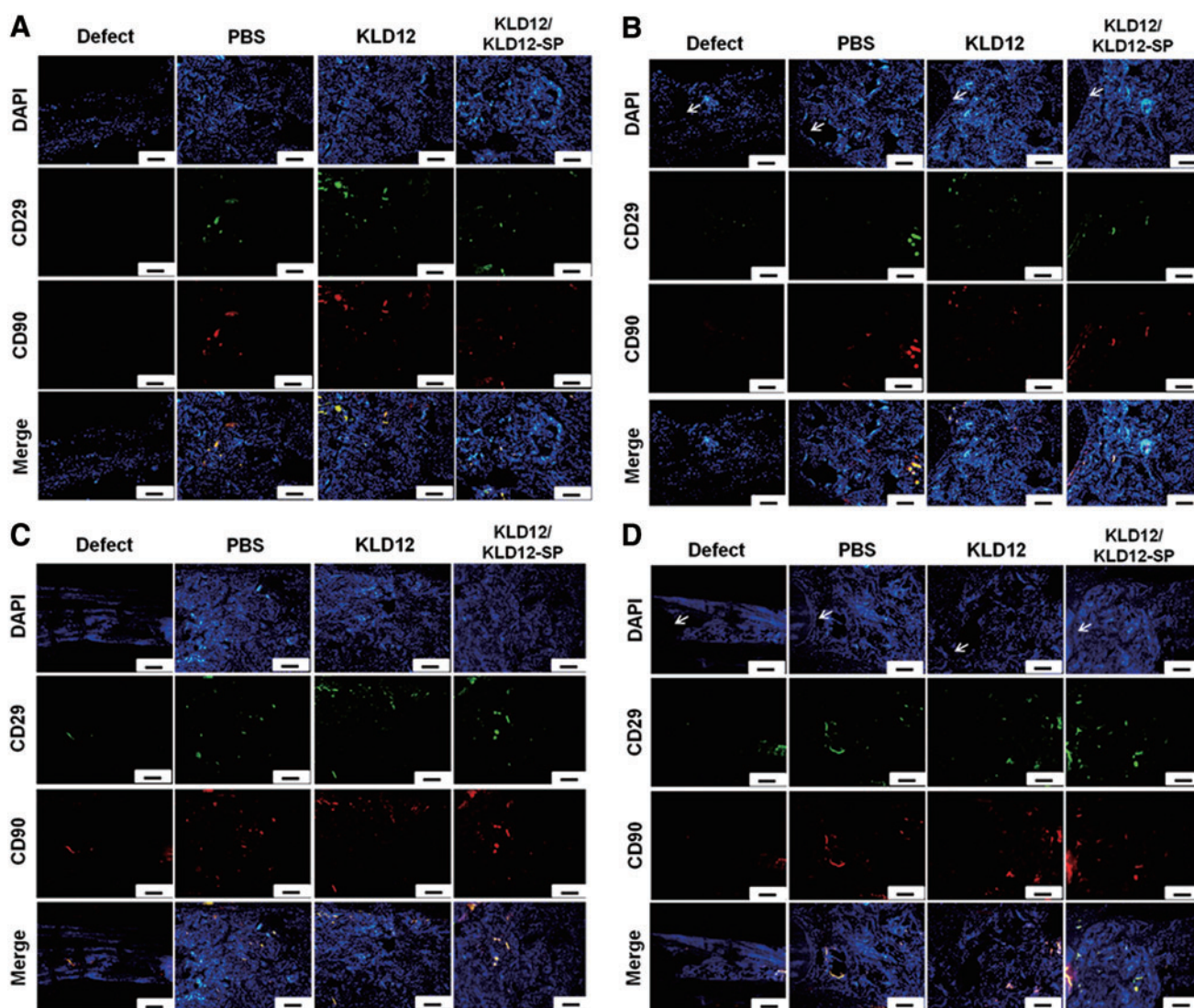


FIG. 6. MSC recruitment of *in vivo* samples. (A) Center at 12 weeks. (B) Edge at 12 weeks. (C) Center at 24 weeks. (D) Edge at 24 weeks (arrow: interface between host and new tissue). Scale bar: 100 μ m. Color images available online at www.liebertpub.com/tea

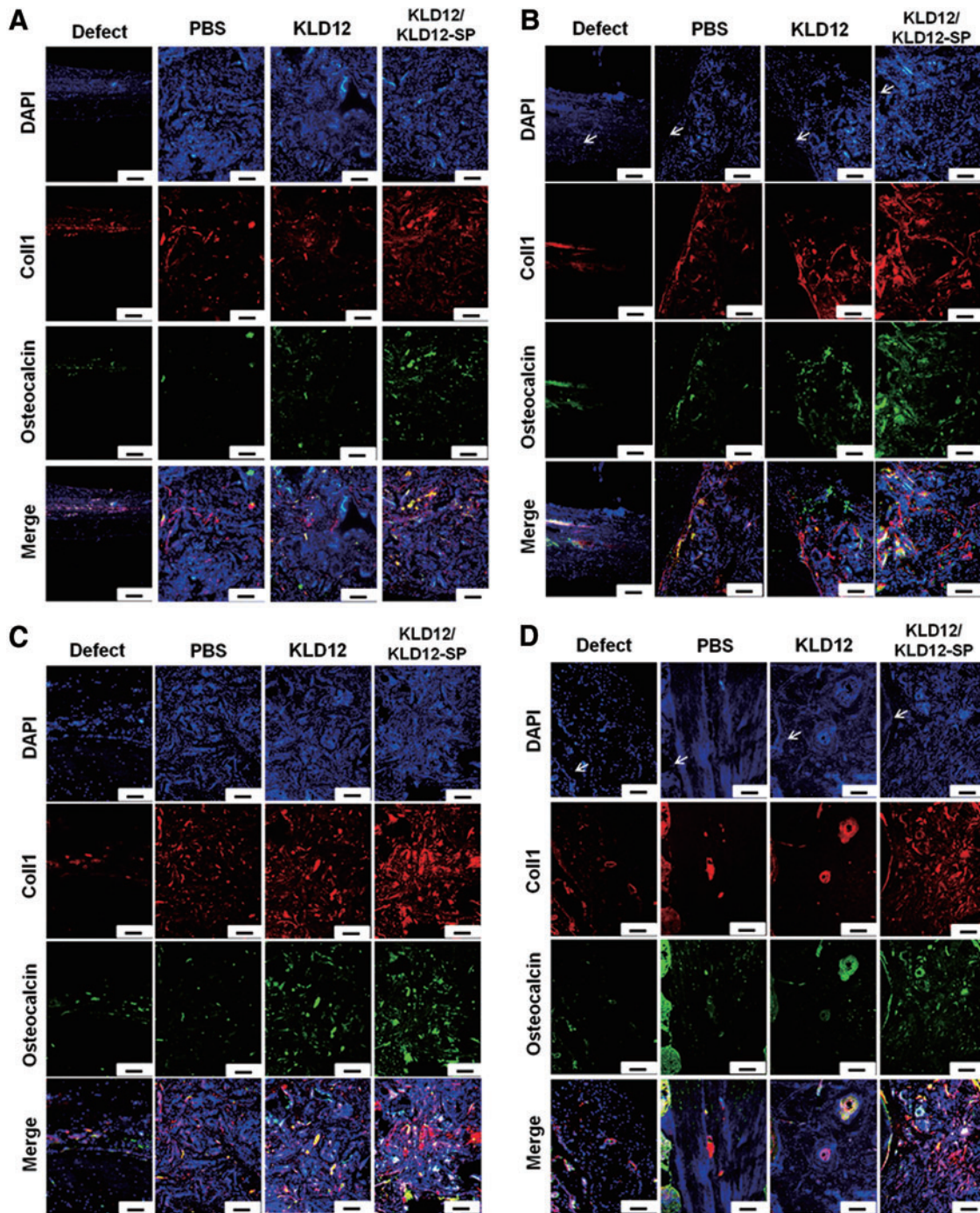


FIG. 7. Immunofluorescence staining of type 1 collagen and osteocalcin. (A) Center at 12 weeks. (B) Edge at 12 weeks. (C) Center at 24 weeks. (D) Edge at 24 weeks (*arrow*: interface between host and new tissue). Scale bar: 100 μ m. Color images available online at www.liebertpub.com/tea

the edge of each sample, relatively more osteoid was observed compared with that of the center. In addition, ECM accumulation was increased over time for the KLD12 and KLD12/KLD12-SP groups. These immunofluorescence staining results were consistent with results from our histological analyses.

From both *in vitro* and *in vivo* MSC recruiting assays, we confirmed that KLD12/KLD12-SP has the ability to recruit MSCs until at least 6 weeks after implantation. Though a

few MSCs were detected in samples from 12 to 24 weeks, new bone tissue formation was enhanced with KLD12/KLD12-SP. The ability of KLD12/KLD12-SP to recruit MSCs in the early phase (within 6 weeks) of wound healing appears to be crucial for enhancing bone regeneration. When MSCs differentiate into specific cells, various proteins are secreted. Type 1 collagen and osteocalcin are essential factors secreted by the MSCs during differentiation into osteoblasts and osteocytes. Type 1 collagen is the main

component of bone that gives its tensile strength by forming oriented layers. Osteocalcin is a specific bone marker, and it acts as an essential linker between the organic parts and mineral components in the bone matrix.^{31–33}

In this study, we added the KLD12/KLD12-SP peptides into the PLA/ β -TCP scaffold for bone tissue regeneration. We confirmed that the β -TCP particles which were exposed on the surface of the scaffolds improved ALP activity and calcium deposition in our previous work.²⁵ Therefore, we expected that recruited MSCs by SP could be differentiated into osteocytes in this system. In the case of vascularized tissues, angiogenesis helps regenerate and maintain the tissue. Numerous studies were reported that SP not only recruited MSCs to the injured site but also enhanced angiogenesis.^{6,8,12–15,17} SP-modified peptide gel (RADA16/RADA16-SP) was applied to a mouse hind limb ischemia model in our previous work in which RADA16/RADA16-SP enhanced angiogenesis and prevented fibrosis and apoptosis in the injured site.⁶ From these studies, we considered that KLD12/KLD12-SP could be a biomaterial for tissue regeneration without cell transplantation.

Conclusion

PLA/ β -TCP scaffold + KLD12/KLD12-SP containing the SP motif at the end of the peptide chain was used to repair flat bone defects without cell transplantation. SP bound to KLD12 acts as a chemo attractant for MSC recruitment. KLD12/KLD12-SP was combined with a PLA/ β -TCP porous scaffold and then applied in a calvarial defect model. From the results, KLD12/KLD12-SP recruited circulating MSCs, leading to accelerated bone tissue formation and repair of the bone defects by the addition of new bone tissue smoothly integrated with host tissue. Consequently, KLD12/KLD12-SP is capable of recruiting MSCs, thus resulting in enhanced tissue regeneration without cell transplantation, which can be utilized in bone tissue engineering by combining this peptide with rigid scaffolds.

Acknowledgments

This work was supported by the KIST Institutional Program (Project No. 2E23720 and 2E25119) and the Seoul R&BD Program (SS110011).

Disclosure Statement

No competing financial interests exist.

References

1. Szpalski, C., Barr, J., Wetterau, M., Saadeh, P.B., and Warren, S.M. Cranial bone defects: current and future strategies. *Neurosurg Focus* **29**, E8, 2010.
2. Elsalanty, M.E., Por, Y.C., Genecov, D.G., Salyer, K.E., Wang, Q., Barcelo, C.R., Troxler, K., Gendler, E., and Opperman, L.A. Recombinant human BMP-2 enhances the effects of materials used for reconstruction of large cranial defects. *J Oral Maxillofac Surg* **66**, 277, 2008.
3. Jung, Y., Kim, S.S., Kim, Y.H., Kim, S.H., Kim, B.S., Kim, S., and Choi, C.Y. A poly(lactic acid)/calcium metaphosphate composite for bone tissue engineering. *Biomaterials* **26**, 6314, 2005.
4. Cowan, C.M., Shi, Y.Y., Aalami, O.O., Chou, Y.F., Mari, C., Thomas, R., Quarto, N., Contag, C.H., Wu, B., and Longaker, M.T. Adipose-derived adult stromal cells heal critical-size mouse calvarial defects. *Nat Biotechnol* **22**, 560, 2004.
5. Zou, D., Zhang, Z., Ye, D., Tang, A., Deng, L., Han, W., Zhao, J., Wang, S., Zhang, W., Zhu, C., Zhou, J., He, J., Wang, Y., Xu, F., Huang, Y., and Jiang, X. Repair of critical-sized rat calvarial defects using genetically engineered bone marrow-derived mesenchymal stem cells overexpressing hypoxia-inducible factor-1 α . *Stem Cells* **29**, 1380, 2011.
6. Kim, J.H., Jung, Y., Kim, B.S., and Kim, S.H. Stem cell recruitment and angiogenesis of neuropeptide substance P coupled with self-assembling peptide nanofiber in a mouse hind limb ischemia model. *Biomaterials* **34**, 1657, 2013.
7. Chen, F.M., Wu, L.A., Zhang, M., Zhang, R., and Sun, H.H. Homing of endogenous stem/progenitor cells for *in situ* tissue regeneration: promises, strategies, and translational perspectives. *Biomaterials* **32**, 3189, 2011.
8. Mauney, J., Olsen, B.R., and Volloch, V. Matrix remodeling as stem cell recruitment event: a novel *in vitro* model for homing of human bone marrow stromal cells to the site of injury shows crucial role of extracellular collagen matrix. *Matrix Biol* **29**, 657, 2010.
9. Ghadge, S.K., Muhlstedt, S., Ozcelik, C., and Bader, M. SDF-1 α as a therapeutic stem cell homing factor in myocardial infarction. *Pharmacol Ther* **129**, 97, 2011.
10. Fong, E.L., Chan, C.K., and Goodman, S.B. Stem cell homing in musculoskeletal injury. *Biomaterials* **32**, 395, 2011.
11. Lau, T.T., and Wang, D.A. Stromal cell-derived factor-1 (SDF-1): homing factor for engineered regenerative medicine. *Expert Opin Biol Ther* **11**, 189, 2011.
12. Hong, H.S., Kim do, Y., Yoon, K.J., and Son, Y. A new paradigm for stem cell therapy: substance-P as a stem cell-stimulating agent. *Arch Pharm Res* **34**, 2003, 2012.
13. Hong, H.S., Lee, J., Lee, E., Kwon, Y.S., Ahn, W., Jiang, M.H., Kim, J.C., and Son, Y. A new role of substance P as an injury-inducible messenger for mobilization of CD29(+) stromal-like cells. *Nat Med* **15**, 425, 2009.
14. Kohara, H., Tajima, S., Yamamoto, M., and Tabata, Y. Angiogenesis induced by controlled release of neuropeptide substance P. *Biomaterials* **31**, 8617, 2010.
15. Dzurik, M.V., Diedrich, A., Black, B., Paranjape, S.Y., Raj, S.R., Byrne, D.W., and Robertson, D. Endogenous substance P modulates human cardiovascular regulation at rest and during orthostatic load. *J Appl Physiol* **102**, 2092, 2007.
16. Abdala, A.P., Haibara, A.S., and Colombari, E. Cardiovascular responses to substance P in the nucleus tractus solitarius: microinjection study in conscious rats. *Am J Physiol Heart Circ Physiol* **285**, H891, 2003.
17. Amadesi, S., Reni, C., Katare, R., Meloni, M., Oikawa, A., Beltrami, A.P., Avolio, E., Cesselli, D., Fortunato, O., Spinetti, G., Ascione, R., Cangiano, E., Valgimigli, M., Hunt, S.P., Emanuelli, C., and Madeddu, P. Role for substance p-based nociceptive signaling in progenitor cell activation and angiogenesis during ischemia in mice and in human subjects. *Circulation* **125**, 1774, 2012.
18. Sun, J., Zheng, Q., Wu, Y., Liu, Y., Guo, X., and Wu, W. Biocompatibility of KLD-12 peptide hydrogel as a scaffold in tissue engineering of intervertebral discs in rabbits. *J Huazhong Univ Sci Technolog Med Sci* **30**, 173, 2010.

19. Sun, J., and Zheng, Q. Experimental study on self-assembly of KLD-12 peptide hydrogel and 3-D culture of MSC encapsulated within hydrogel *in vitro*. *J Huazhong Univ Sci Technolog Med Sci* **29**, 512, 2009.
20. Zhang, S., Marini, D.M., Hwang, W., and Santoso, S. Design of nanostructured biological materials through self-assembly of peptides and proteins. *Curr Opin Chem Biol* **6**, 865, 2002.
21. Caplan, M.R., Moore, P.N., Zhang, S., Kamm, R.D., and Lauffenburger, D.A. Self-assembly of a beta sheet protein governed by relief of electrostatic repulsion relative to van der Waals attraction. *Biomacromolecules* **1**, 627, 2000.
22. Zhang, S., Lockshin, C., Cook, R., and Rich, A. Unusually stable beta-sheet formation in an ionic self-complementary oligopeptide. *Biopolymers* **34**, 663, 1994.
23. Kisiday, J., Jin, M., Kurz, B., Hung, H., Semino, C., Zhang, S., and Grodzinsky, A.J. Self-assembling peptide hydrogel fosters chondrocyte extracellular matrix production and cell division: implications for cartilage tissue repair. *Proc Natl Acad Sci U S A* **99**, 9996, 2002.
24. Benoit, D.S., Schwartz, M.P., Durney, A.R., and Anseth, K.S. Small functional groups for controlled differentiation of hydrogel-encapsulated human mesenchymal stem cells. *Nat Mater* **7**, 816, 2008.
25. Jung, Y., Part, M.S., Kim, S.S., Kim, B.S., Kim, Y.H., Kim, S.-H., Lee, J.W., and Kim, S.H. Reconstruction of a rabbit ulna bone defect using bone marrow stromal cells and a PLA/ β -TCP composite by a novel sintering method. *Adv Eng Mater* **11**, 169, 2009.
26. Qiu, Q., Basak, A., Mbikay, M., Tsang, B.K., and Gruslin, A. Role of pro-IGF-II processing by proprotein convertase 4 in human placental development. *Proc Natl Acad Sci U S A* **102**, 11047, 2005.
27. Walsh, W.R., Vizesi, F., Michael, D., Auld, J., Langdown, A., Oliver, R., Yu, Y., Irie, H., and Bruce, W. Beta-TCP bone graft substitutes in a bilateral rabbit tibial defect model. *Biomaterials* **29**, 266, 2008.
28. Ramaswamy, Y., Haynes, D.R., Berger, G., Gildenhaar, R., Lucas, H., Holding, C., and Zreiqat, H. Bioceramics composition modulate resorption of human osteoclasts. *J Mater Sci Mater Med* **16**, 1199, 2005.
29. Habibovic, P., and de Groot, K. Osteoinductive biomaterials—properties and relevance in bone repair. *J Tissue Eng Regen Med* **1**, 25, 2007.
30. Burdon, T.J., Paul, A., Noiseux, N., Prakash, S., and Shum-Tim, D. Bone marrow stem cell derived paracrine factors for regenerative medicine: current perspectives and therapeutic potential. *Bone Marrow Res* **2011**, 207326, 2011.
31. Aubin, J.E., Liu, F., Malaval, L., and Gupta, A.K. Osteoblast and chondroblast differentiation. *Bone* **17**, 77S, 1995.
32. Delmas, P.D., Demiaux, B., Malaval, L., Chapuy, M.C., and Meunier, P.J. Osteocalcin (or bone gla-protein), a new biological marker for studying bone pathology. *Presse Med* **15**, 643, 1986.
33. Roach, H.I. Why does bone matrix contain non-collagenous proteins? The possible roles of osteocalcin, osteonectin, osteopontin and bone sialoprotein in bone mineralisation and resorption. *Cell Biol Int* **18**, 617, 1994.

Address correspondence to:

Tae Hyun Choi, MD, PhD

Department of Plastic and Reconstructive Surgery

Institute of Human-Environment Interface Biology

Institute of Dermatologic Science

College of Medicine

Seoul National University

Seoul 110-799

Korea

E-mail: psthchoi@snu.ac.kr

Youngmee Jung, PhD

Department of Biomedical Engineering

University of Science and Technology (UST)

Seoul 136-791

Korea

E-mail: winnie97@kist.re.kr

Received: August 6, 2014

Accepted: November 18, 2014

Online Publication Date: January 9, 2015